

# A Study of the Truncated Square Pyramid Geometry for Enhancement of Super-hydrophobicity

Wei Gong<sup>1,2</sup>, Yangang Wang<sup>1</sup>, Yiyi Chen<sup>1</sup>, Xiang Li<sup>1</sup>, Kongjing Li<sup>1</sup>, Zhongxu Wang<sup>1</sup>, Yuying Yan<sup>2\*</sup>

1. R&D Centre: Semiconductors, Dynex Semiconductor Ltd. Doddington Road, Lincoln, LN6 3LF, UK

2. Fluids and Thermal Engineering Research Group, Faculty of Engineering, University of Nottingham, Nottingham, NG7 2RD, UK

## Abstract

Super-hydrophobic surfaces are quite common in nature, inspiring people to continually explore its water-repellence property and applications to our lives. It has been generally agreed that the property of super-hydrophobicity is mainly contributed by the microscale or nanoscale (or even smaller) architecture on the surface. Besides, there is an energy barrier between the Cassie-Baxter wetting state and the Wenzel wetting state. An optimized square post micro structure with truncated square pyramid geometry is introduced in this work to increase the energy barrier, enhancing the robustness of super-hydrophobicity. Theoretical analysis is conducted based on the wetting transition energy curves. Numerical simulation based on a phase-field lattice Boltzmann method is carried out to verify the theoretical analysis. The numerical simulation agrees well with the theoretical analysis, showing the positive significance of the proposed micro structure. Furthermore, another novel micro structure of rough surface is presented, which combines the advantages of truncated pyramid geometry and noncommunicating roughness elements. Theoretical analysis shows that the novel micro structure of rough surface can effectively hinder the Cassie-Baxter state to Wenzel state transition, furtherly enhancing the robustness of the surface hydrophobicity.

**Keywords:** truncated square pyramid geometry, wetting transition, energy barrier, super-hydrophobicity, lattice Boltzmann method

Copyright © Jilin University 2020.

## 1 Introduction

Hydrophobic surfaces are quite common in natural surfaces from both animals and plants, for example, dragonfly wings, bird feathers, water strider feet, rose petal surface, as well as the well-known lotus leaves. People usually use the lotus effect to refer to the water-repellence or self-cleaning properties of lotus leaves, which thus has been a typical natural super-hydrophobicity example for researchers to study wettability and hydrophobicity. It has been found that the extreme high water-repellence of such surfaces is mainly contributed by the microscale or nanoscale (or even smaller) architecture on the surface, more precisely, on the rough surface, which changes the surface free energy of the water droplet, minimizing the adhesion between the droplet and the surface<sup>[1]</sup>. In recent years, the study of fluid droplets interactions with superhydrophobic surfaces has been more and more popular, involving a number of cutting-edge topics in engineering and bio-

tech research areas. Studies of hydrophobicity have been branched in fundamental research such as surface structures<sup>[2]</sup>, physical and chemical properties<sup>[3,4]</sup>, fluid flow<sup>[5]</sup>, and engineering applications including anti-icing<sup>[6]</sup>, boiling heat transfer<sup>[7]</sup>, self-cleaning<sup>[8]</sup>, printing<sup>[9]</sup>, painting<sup>[10]</sup>, etc.

The main wetting states mainly include Cassie-Baxter wetting state<sup>[11]</sup>, Wenzel wetting state<sup>[12]</sup>, impregnating wetting state<sup>[13]</sup> and a mushroom wetting state<sup>[14]</sup>, of which the Cassie-Baxter wetting state and Wenzel wetting state are more common. Cassie-Baxter wetting state means the droplet sits upon the micro/nano structures, with air pockets bounded between the surface and droplet; while for Wenzel wetting state, the air pockets space is penetrated with water liquid, no air between the droplet and the surface. There is an energy barrier between Cassie-Baxter wetting state and Wenzel wetting state, therefore on the same homogeneous surface, the two wetting states can coexist<sup>[15]</sup>. In such a scenario, the Cassie-Baxter wetting state presents a

\*Corresponding author: Yuying Yan  
E-mail: [yuying.yan@nottingham.ac.uk](mailto:yuying.yan@nottingham.ac.uk)

higher apparent contact angle. The energy barrier can be overcome by external energy such as pressure, initial speed, vibration, electric field, or even gravity. Investigation into the mechanism of wetting transitions is of great importance for designing and manufacturing super-hydrophobic surfaces. Wetting transitions have been studied theoretically, numerically and experimentally. Bormashenko<sup>[16,17]</sup> did review work on the main experimental and theoretical studies on wetting transitions, and concluded that the most efficient approach to increase the energy barrier is to reduce the microstructural scales. Patankar<sup>[18]</sup> studied the wetting transition theoretically based on the energy balance with Cassie's wetting law<sup>[19]</sup> and Wenzel's wetting law<sup>[20]</sup>, to determine the possibility of wetting transition occurrence. The energy barrier is also discussed in his study. Our previous study<sup>[21]</sup> theoretically analyzed the wetting transition surface free energy variance according to the transition processes as well as the intermediate wetting energy curves for different intrinsic Young's angles. Numerical simulation using a mesoscale multiphase flow method, phase-field lattice Boltzmann method, was implemented to study the wetting transition process and validate the proposed wetting transition energy curves<sup>[22]</sup>. Dufour *et al.*<sup>[23]</sup> and Tuteja *et al.*<sup>[24,25]</sup> experimentally studied the reentrant structure for superomniphobic surfaces to low surface tension liquids. Liu and Kim<sup>[2]</sup> proposed a rough surface with a specific doubly re-entrant structure, and the experiment study showed the surface with such structure made from a completely wettable material could be truly superomniphobic even to extremely low-energy liquid perfluorohexane. Bahadur and Garimella<sup>[26]</sup> worked on the artificially structured surface with non-communicating roughness elements (closed cell), which could enhance the robustness of the Cassie-Baxter state and significantly hinder the transition with external forces.

The aim of this work is to study the effect on wetting transition from Cassie-Baxter wetting state to Wenzel wetting state of rough surface with patterned truncated pyramid geometry posts, as shown in Fig. 1, both theoretically and numerically, which is helpful to understand the wetting transitions mechanism and explore the higher quality and high performance

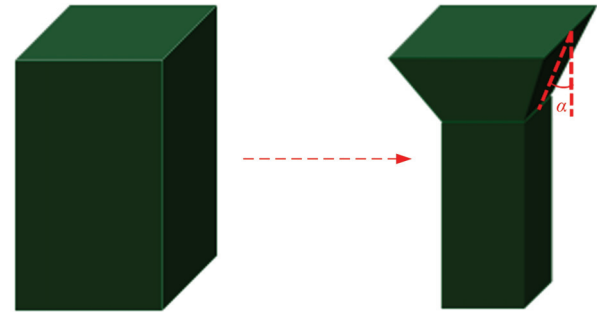


**Fig. 1** Optimizing the micro square post to the post with truncated square pyramid geometry.

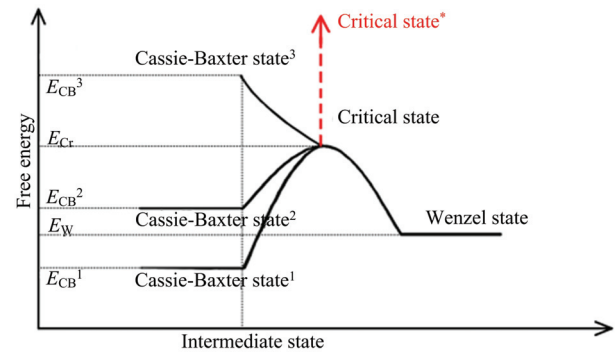


**Fig. 2** Raising the critical state free energy and the energy barrier.

super-hydrophobic surfaces.

## 2 Theoretical analysis

To improve the stability of hydrophobic surfaces, the micro square post is optimized to the post with truncated square pyramid geometry, as shown in Fig. 1. The theoretical analysis follows our previous study<sup>[21]</sup> with the proposed energy curves in Fig. 2. For the intermediate state when the transition occurs with square posts (Fig. 3a in Ref. [21]), the free energy can be given as:

$$\tilde{E}_{CB} = \tilde{S}_{CB} \left\{ \left[ f + (r-1) \frac{h'}{h} \right] (\sigma_{SL} - \sigma_{SG}) + (1-f) \sigma_{LG} \right\} + \tilde{S}'_{CB} \sigma_{LG}, \tag{1}$$

where  $\tilde{E}_{CB}$  is the intermediate wetting state free energy,  $\tilde{E}_{CB}$  is the intermediate projected solid/liquid interface area (refer to Fig. 2b in Ref. [21]),  $\tilde{S}'_{CB}$  is the liquid/gas interface area around the water droplet (refer to Fig. 2c in Ref. [21]),  $f$  is the area fraction of the projected solid/liquid contact area over the total projected solid/liquid and liquid/gas area,  $r$  is the ratio of the actual surface area over the projected surface area,  $h$  is the

height of the square post,  $h'$  is the water droplet penetrated depth (Fig. 3a in Ref. [21]), and  $\sigma_{SL}$ ,  $\sigma_{SG}$  and  $\sigma_{LG}$  are the surface tension between solid/liquid, solid/gas and liquid/gas, respectively. In Eq. (1) the term  $\tilde{S}_{CB} \{f(\sigma_{SL} - \sigma_{SG}) + (1 - f)\sigma_{LG}\} + \tilde{S}'_{CB}\sigma_{LG}$  after expansion is the Cassie-Baxter wetting state free energy; while the term  $\tilde{S}_{CB}(r - 1)\frac{h'}{h}(\sigma_{SL} - \sigma_{SG})$  after expansion represents the increased free energy while transitioning, which is proportional to the increased solid/fluid contact area  $\tilde{S}_{CB}(r - 1)\frac{h'}{h}$ . In the optimized micro structure with truncated square pyramid geometry, for the same penetration depth  $h'$ , the increased solid/fluid contact area can be written as  $\tilde{S}_{CB}(r - 1)\frac{h'}{h \cdot \cos \alpha^*}$ , where  $\alpha^*$  is an equivalent dip angle to the dip angle  $\alpha$  shown in Fig. 1 considering the four oblique surfaces of the square pyramid geometry, and  $\alpha^*$  can be obtained *via* simple geometry calculations from  $\alpha$ . Therefore, the free energy of the intermediate wetting transition state on the pyramid side surface for the proposed truncated square pyramid geometry can then be given by Eq. (2).

For the same penetration depth, the free energy  $\tilde{E}_{CB}^*$  in Eq. (2) is apparently higher than  $\tilde{E}_{CB}$  in Eq. (1), indicating that the slope of the transition energy curve from Cassie-Baxter state to critical state as well as the critical state free energy of the proposed geometry are higher than those of the general square post geometry, and the critical state free energy is raised up as shown in Fig. 2.

In Fig. 2, the black solid curves are the energy curves for the general square posts structure. Cassie-Baxter state<sup>1</sup> and Cassie-Baxter state<sup>2</sup> stand for the stable state (having lower free energy than Wenzel state) and metastable state (having higher free energy than Wenzel state) for intrinsic Young's angle greater than 90°. Cassie-Baxter state<sup>3</sup> represents the scenario where the

intrinsic Young's angle for the substrate and the droplet is smaller than 90°, and the Cassie-Baxter state theoretically does not exist. By adopting the optimized micro structure with truncated square pyramid geometry, the critical state free energy is increased (red dotted line in Fig. 2), which could be even higher than that of Cassie-Baxter state<sup>3</sup>, which means the Cassie-Baxter wetting state can exist on a patterned rough surface of which the intrinsic Young's angle is smaller than 90°.

### 3 Numerical simulation and discussion

The same numerical method for simulation used in our previous study<sup>[22]</sup>, a D3Q15 phase-field lattice Boltzmann method for a large density ratio is adopted to carry out the numerical verification of the above theoretical analysis. Eqs. (3) and (4) are the main governing equilibrium distribution function equations involving the streaming and collision steps of fluid particles to simulate the multiphase fluid flow in mesoscale. Details about the numerical method can be found in Ref. [22].

Validation of the numerical method was complemented by comparing the numerical simulation results and theoretical values. The apparent contact angles of water droplets on a smooth flat surface and square posts patterned surface from simulation were in good agreement with the calculated contact angles from the Young equation, the Cassie-Baxter equation and the Wenzel equation. Details of the numerical method validation can

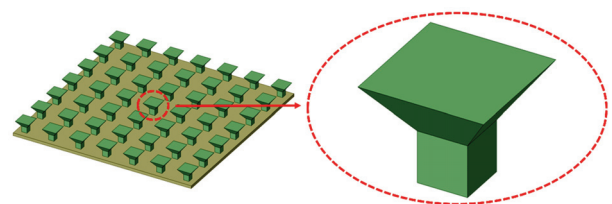


**Fig. 3** Patterned rough surface with truncated square pyramid posts.

$$\tilde{E}_{CB}^* = \tilde{S}_{CB} \left\{ \left[ f + (r - 1) \frac{h'}{h \cdot \cos \alpha^*} \right] (\sigma_{SL} - \sigma_{SG}) + (1 - f) \sigma_{LG} \right\} + \tilde{S}'_{CB} \sigma_{LG} \tag{2}$$

$$f_\alpha(\mathbf{x} + \mathbf{c}_\alpha \delta_t, t + \delta_t) = f_\alpha(\mathbf{x}, t) - \frac{1}{\tau_f} (f_\alpha(\mathbf{x}, t) - f_\alpha^{eq}(\mathbf{x}, t)), \tag{3}$$

$$g_\alpha(\mathbf{x} + \mathbf{c}_\alpha \delta_t, t + \delta_t) = g_\alpha(\mathbf{x}, t) - \frac{1}{\tau_g} (g_\alpha(\mathbf{x}, t) - g_\alpha^{eq}(\mathbf{x}, t)) + 3\omega_\alpha \frac{1}{\rho} \nabla \cdot [\mu(\nabla \mathbf{u} + \mathbf{u}\nabla)]. \tag{4}$$

be found in Ref. [22] as well.

The simulation settings are similar to the simulation settings in Ref. [22], where just the square posts are replaced by the optimized micro structure with truncated square pyramid geometry, as shown in Fig. 3. The top surface of each post is  $5 \mu\text{m} \times 5 \mu\text{m}$ , the posts are patterned every  $10 \mu\text{m}$  in two dimensions and the dip angle of the pyramid side surfaces is  $45^\circ$ . The height of the posts and the lower square post part do not matter in this study as the study is just focused on the effect from the pyramid oblique side surfaces. Other settings except the intrinsic Young's angle are kept the same with Ref. [22].

A comparison between the general square posts and the optimized posts with truncated square pyramid geometry is firstly conducted. Both of the droplets are released above the substrate with a certain distance, bringing about an initial speed to go against the energy barrier. The intrinsic Young's angle is  $115^\circ$ , and all other simulation settings except the micro structures are the same. The simulation results are shown in Fig. 4, where

it can be clearly seen that Wenzel wetting state is formed for the square posts, while Cassie-Baxter wetting state is achieved on the optimized surface. The results show the optimized surface has a higher critical free energy than the square posts. The dynamic wetting process for the optimized structure is presented in Fig. 5. The simulation results are given in 2D cross-section view, but the simulation is in 3D. It should be noted here that to study the wetting process on a rough surface, 2D simulation is not

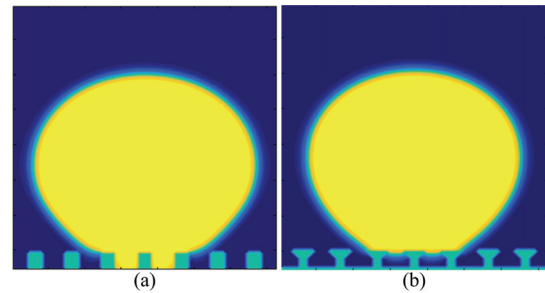


**Fig. 4** Steady state of a water droplet with initial speed on patterned micro rough surface,  $\theta_Y = 105^\circ$ . (a) Square posts; (b) optimized posts with truncated square pyramid geometry.

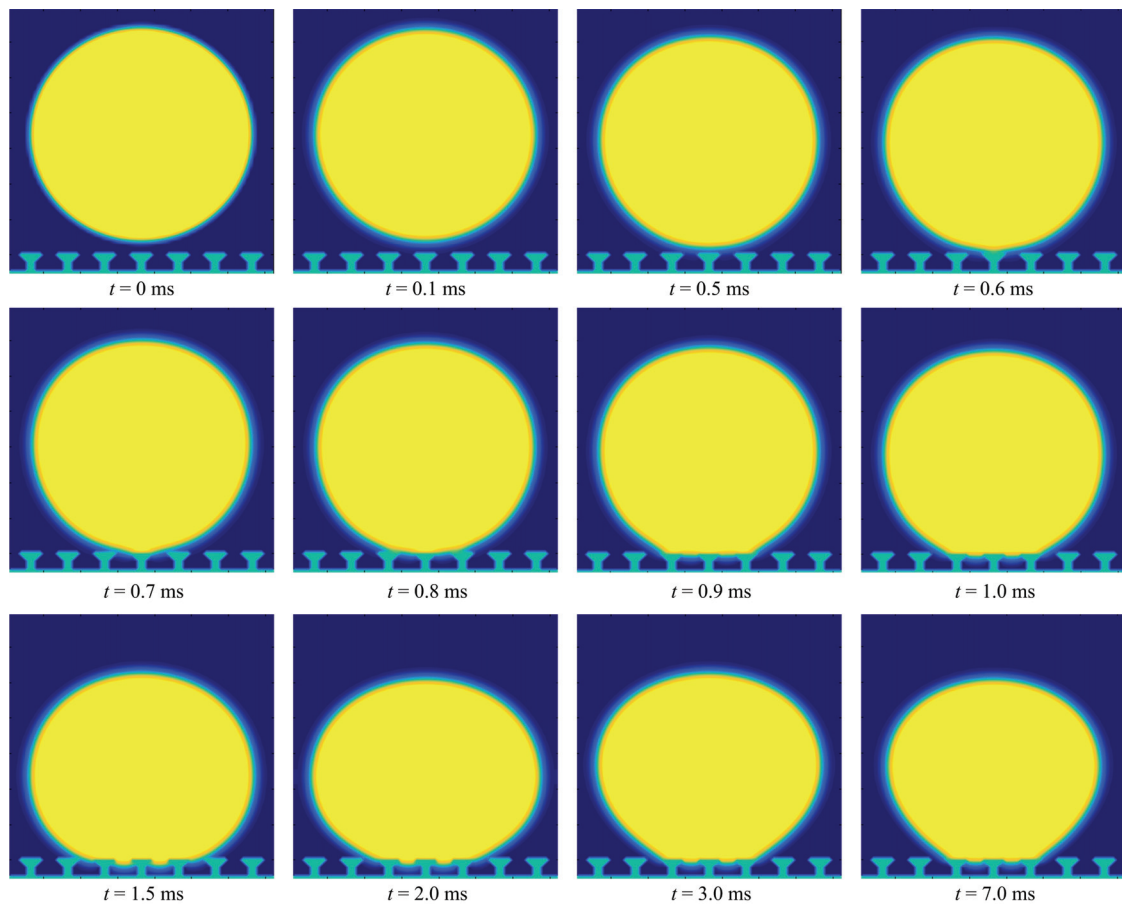


**Fig. 5** Water droplet motion on the optimized micro rough surface,  $\theta_Y = 105^\circ$ .

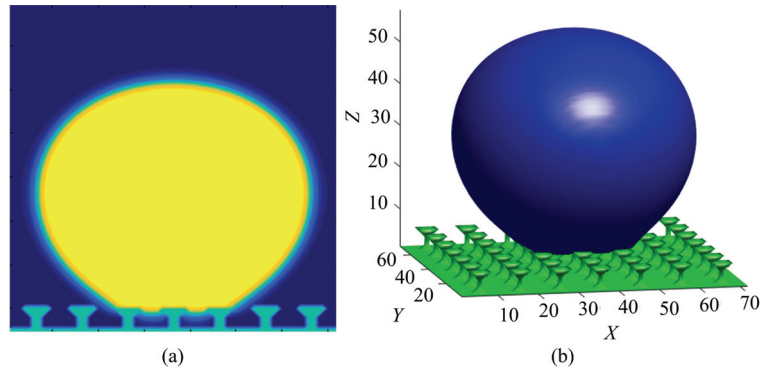


**Fig. 6** Steady state of a water droplet with initial speed on the optimized patterned micro rough surface,  $\theta_y = 81^\circ$ . (a) 2D view; (b) 3D view.

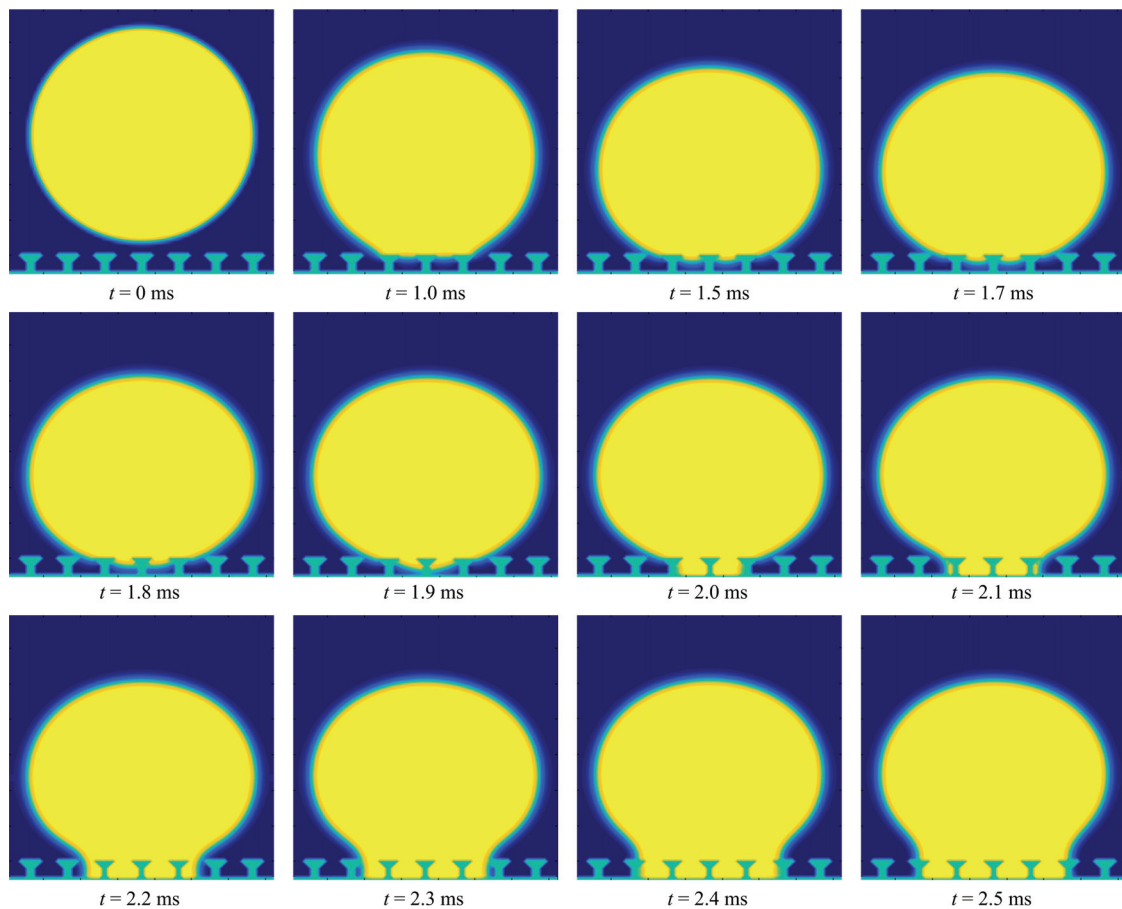


**Fig. 7** Water droplet motion on the optimized micro rough surface,  $\theta_y = 80^\circ$ .

applicable, though it can be seen in some studies. Because for a 2D simulation of Cassie-Baxter wetting state, the air trapped between the droplet and the surface is truly trapped, however in 3D simulation, the air beneath the droplet is still able to flow as it is open to the outer environment. This can be easily figured out in Fig. 6.

Fig. 6 shows a steady wetting state after the water droplet reached the rough surface in 2D view and 3D

view. The intrinsic Young's angle in this case is  $81^\circ$ , smaller than  $90^\circ$ , while it can be clearly seen that the steady wetting state is Cassie-Baxter state, which means there is an energy barrier and the critical free energy is higher than the Cassie-Baxter state<sup>3</sup> free energy in Fig. 2.

However, when the intrinsic Young's angle is set as  $80^\circ$ , the wetting transition from Cassie-Baxter state to Wenzel state occurs. As shown in Fig. 7, the air pockets

**Table 1** Tested intrinsic Young's angle and the corresponding steady wetting state

Tested intrinsic Young's angle	75°	77°	80°	81°	85°	105°
Steady wetting state	Wenzel	Wenzel	Wenzel	Cassie-Baxter	Cassie-Baxter	Cassie-Baxter

surrounding the posts are driven away and the water penetrates into the micro structure space. The water droplet reaches the bottom surface at around 2 ms and continues to penetrate the micro structure afterwards.

Six groups simulation were conducted to investigate the relationship between the intrinsic Young's angle and the steady wetting state. The test results are given in Table 1. The minimum intrinsic Young's angle for a steady Cassie-Baxter wetting state is 81° in this simulation work.

For the pyramid geometry, there is always a potential on the oblique side surfaces to drive the water droplet back to Cassie-Baxter wetting state, making a reverse transition possible; while for the T-shape or doubly re-entrant geometry, once the energy barrier is overcome, the reverse transition hardly happens.

It should be noted that one of the advantages of numerical study compared with experimental study is that the effect of structures with a smaller scale than the main patterned micro/nano structure can be eliminated, thus to have a better understanding of the mechanism of wetting transitions.

#### 4 A novel design

A novel design combining the advantages of both truncated pyramid geometry structure and the noncommunicating roughness elements micro structure is shown in Fig. 8. The advantage of noncommunicating elements structure is that the air pockets is truly trapped between the water droplet and the substrate surface to stop the further penetration to Wenzel state. While the oblique surfaces of the truncated square pyramid would give the droplet the force to move upwards, when the intrinsic Young's angle is greater than a certain value as discussed above. Therefore, potentially this novel design has better stability for super-hydrophobicity, since even the external force overcomes the energy barrier caused by the pyramid geometry, the micro walls between the posts could still stop the further penetration to Wenzel wetting state. However, the thickness of the micro walls should be thin enough so the energy of adhesion between

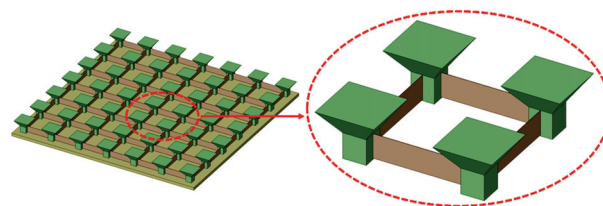


**Fig. 8** The proposed novel micro structure of rough surface with walls between the optimized posts.

the droplet and the top of the walls can be potentially overcome by the force provided by the oblique surfaces. Numerically simulation is difficult to be conducted for such a multi-scale scenario. This design needs further study with a better numerical approach for multi-scale simulation or experimental investigation.

#### 5 Conclusion

The effect of rough surface with truncated square pyramid geometry posts on wetting transition from Cassie-Baxter wetting state to Wenzel wetting state is studied both theoretically and numerically in this paper. Theoretical analysis is based on the wetting transition energy curves proposed in our previous study. The numerical simulation with mesoscale multiphase flow method, phase-field lattice Boltzmann method, is validated with theoretical data for water droplets wetting motions on both smooth flat surface and patterned micro structure surface. The numerical simulation results show a good agreement with the theoretical analysis. Numerically study of water droplets motions on surfaces with truncated square pyramid geometry posts with different intrinsic Young's angles is carried out to study the wetting properties. The wetting transition from Cassie-Baxter wetting state to Wenzel wetting state with a lower intrinsic Young's angle material with the proposed micro structure is presented. In addition, a novel micro structure of rough surface which combines the advantages of both truncated pyramid geometry structure and the noncommunicating roughness elements micro structure is proposed in this paper. Theoretical analysis is conducted on this novel micro structure. Through this study, the following conclusions can be made:

(1) Theoretically, the inverted pyramid geometry (oblique surfaces), compared with square posts with vertical side faces, can increase the critical wetting transition state free energy, enhancing the stability of super-hydrophobic surface water repellence.

(2) The numerical simulation verified the theoretical analysis, and shows stable Cassie-Baxter wetting states when the Young's angle is less than  $90^\circ$ .

(3) The proposed novel micro structure with both pyramid geometry and noncommunicating roughness elements theoretically presents even better water repellence and super-hydrophobicity stability, to stop the formation of Wenzel wetting state.

## Acknowledgment

This work is supported by European Union project H2020 - MSCA - RISE 778104.

## References

- [1] Yan Y Y, Gao N, Barthlott W. Mimicking natural superhydrophobic surfaces and grasping the wetting process: A review on recent progress in preparing superhydrophobic surfaces. *Advances in Colloid and Interface Science*, 2011, **169**, 80–105.
- [2] Liu T, Kim C J. Turning a surface superrepellent even to completely wetting liquids. *Science*, 2014, **346**, 1096–1100.
- [3] Li Q Z, Lin B Q, Zhao S, Dai H M. Surface physical properties and its effects on the wetting behaviors of respirable coal mine dust. *Powder Technology*, 2013, **233**, 137–145.
- [4] Wagh P B, Ingale S V. Comparison of some physico-chemical properties of hydrophilic and hydrophobic silica aerogels. *Ceramics International*, 2002, **28**, 43–50.
- [5] Khojasteh D, Mousavi S M, Kamali R. CFD analysis of Newtonian and non-Newtonian droplets impinging on heated hydrophilic and hydrophobic surfaces. *Indian Journal of Physics*, 2017, **91**, 513–520.
- [6] Farhadi S, Farzaneh M, Kulinich S A. Anti-icing performance of superhydrophobic surfaces. *Applied Surface Science*, 2011, **257**, 6264–6269.
- [7] Betz A R, Xu J, Qiu H, Attinger D. Do surfaces with mixed hydrophilic and hydrophobic areas enhance pool boiling? *Applied Physics Letters*, 2010, **97**, 2012–2015.
- [8] Kapridaki C, Maravelaki-Kalaitzaki P. TiO<sub>2</sub>-SiO<sub>2</sub>-PDMS nano-composite hydrophobic coating with self-cleaning properties for marble protection. *Progress in Organic Coatings*, 2013, **76**, 400–410.
- [9] Campos D F D, Blaeser A, Weber M, Jäkel J, Neuss S, Jähnen-Dechent W, Fischer H. Three-dimensional printing of stem cell-laden hydrogels submerged in a hydrophobic high-density fluid. *Biofabrication*, 2013, **5**, 015003.
- [10] Gui O M, Cîntă Pînzaru S. Hydrophobic painting materials fast detection using temperature dependence SERS on simple or PEGylated Ag nanoparticles. *Dyes and Pigments*, 2017, **146**, 551–557.
- [11] Cassie A B D, Baxter S. Wettability of porous surfaces. *Transactions of the Faraday Society*, 1944, **40**, 546–551.
- [12] Wenzel R N. Surface roughness and contact angle. *The Journal of Physical Chemistry*, 1949, **53**, 1466–1467.
- [13] Bormashenko E, Pogreb R, Stein T, Whyman G, Erlich M, Musin A, Machavariani V, Aurbach D. Characterization of rough surfaces with vibrated drops. *Physical Chemistry Chemical Physics*, 2008, **10**, 4056–4061.
- [14] Ishino C, Okumura K. Wetting transitions on textured hydrophilic surfaces. *European Physical Journal E*, 2008, **25**, 415–424.
- [15] He B, Patankar N A, Lee J. Multiple equilibrium droplet shapes and design criterion for rough hydrophobic surfaces. *Langmuir*, 2003, **19**, 4999–5003.
- [16] Bormashenko E. Wetting transitions on biomimetic surfaces. *Philosophical Transactions of the Royal Society A: Mathematical, Physical and Engineering Sciences*, 2010, **368**, 4695–4711.
- [17] Bormashenko E. Progress in understanding wetting transitions on rough surfaces. *Advances in Colloid and Interface Science*, 2015, **222**, 92–103.
- [18] Patankar N A. Transition between superhydrophobic states on rough surfaces. *Langmuir*, 2004, **20**, 7097–7102.
- [19] Cassie A B D. Contact angles. *Discussions of the Faraday society*, 1948, **3**, 11–16.
- [20] Marmur A. Wetting on hydrophobic rough surfaces: To be heterogeneous or not to be? *Langmuir*, 2003, **19**, 8343–8348.
- [21] Gong W, Zu Y Q, Chen S, Yan Y Y. Wetting transition energy curves for a droplet on a square-post patterned surface. *Science Bulletin*, 2017, **62**, 136–142.
- [22] Gong W, Yan Y Y, Chen S, Giddings D. Numerical study of wetting transitions on biomimetic surfaces using a lattice boltzmann approach with large density ratio. *Journal of Bionic Engineering*, 2017, **14**, 486–496.
- [23] Dufour R, Perry G, Harnois M, Coffinier Y, Thomy V, Senez V, Boukherroub R. From micro to nano reentrant structures: Hysteresis on superomniphobic surfaces. *Colloid and Po-*

- lymer Science*, 2013, **291**, 409–415.
- [24] Tuteja A, Choi W, Mabry J M, McKinley G H, Cohen R E. Robust omniphobic surfaces. *Proceedings of the National Academy of Sciences of the United States of America*, 2008, **105**, 18200–18205.
- [25] Tuteja A, Choi W, McKinley G H, Cohen R E, Rubner M F. Design parameters for superhydrophobicity and superoleophobicity. *MRS Bulletin*, 2008, **33**, 752–758.
- [26] Ma M, Hill R M. Superhydrophobic surfaces. *Current Opinion in Colloid and Interface Science*, 2006, **11**, 193–202.